## Response

### A. Introduction

Claims 1-21 remain pending in the application. Although the Office Action is inconsistent (as to claim 4) and unclear (as to claims 2, 7-9, and 11-12), the Examiner seems to have rejected claims 1-2, 4, 7-9, and 11 under 35 U.S.C. § 102(b) as anticipated by U.S. Patent No. 5,711,888 to Trampler, et al. and claims 3, 10, 12, and 20 under 35 U.S.C. § 103(a) as obvious over the combined disclosures of the Trampler patent and an article from *Sensors and Actuators* entitled "Force Field Particle Filter, Combining Ultrasound Standing Waves and Laminar Flow," by J. Hawkes, et al. (the "Hawkes 1 Article"). The Examiner also objects to claim 8 because it supposedly is "a little unclear" and to claim 11 because of its misspelling of "ultrasound." According to the Examiner, claims 5-6, 13-18, and 21 would be allowable if appropriately rewritten.

### B. Claim Objections

Responding to the Examiner's objections, Applicants have revised claim 11 to correct the spelling of the word "ultrasound." Respecting claim 8, Applicants cannot locate any unclear portion and believe the Examiner's objection as to that claim is erroneous. Applicants accordingly request that the Examiner's objections to the claims be withdrawn.

### C. Claim Rejections

As recited in claim 1, Applicants' invention comprises an apparatus for directing particles entrained in a fluid, including a chamber having first and second walls, with the second wall capable of reflecting a sound wave and having a thickness

such that the path length of the standing wave in the second wall is a multiple of about ½ the wavelength $\lambda_T$ of the sound wave therein.

Independent claim 19 is similar in this respect. Configuring thickness of the second wall as recited in these claims allows creation of a pressure node at the interface of the fluid and second wall, which is required for directing articles to the interface. See, e.g., Application at p. 4, l. 13 through p. 5, l. 7.

In rejecting these independent claims, the Examiner has misconstrued the disclosure of the Trampler patent. Without ***any*** support whatsoever, the Examiner defines the path length of a standing wave of the Trampler patent to be "equal to [the] distance the standing wave travels through the mirror layer and then through the mirror layer again as it is echoed or reflected back." See Office Action at p. 3. This definition, however, is clearly incorrect.

A standing wave may be produced when a sound wave transmitted from a first wall is superimposed by the sound wave reflected from a second wall and is characterized by the wave appearing to be "standing still." In reality, though, the sound wave is continuously propagated between the first and second walls. However, the path length of the standing wave is ***not*** the sum of the many (unknown) number of times the wave propagates between the two walls--much less the sum of a single cycle of the wave as the Examiner arbitrarily contends.

Instead, the path length of a standing wave is in fact the end-to-end distance, or length, of the wave. The path length is therefore equivalent to the thickness of the medium through which it propagates (*i.e.* "path length" and "thickness" are interchangeable in this respect). This definition is consistent with

Applicants' disclosure. Cf. Application at p. 14, l. 15 through p. 15, l. 10 (compare descriptive text with Table 1); see also id. at p. 6, ll. 17-22; p. 8, ll. 10-14. It also is well understood by those skilled in the appropriate art. See, e.g., J. Hawkes, et al., "Microparticle Manipulation in Millimetre Scale Ultrasonic Standing Wave Chambers," *Ultrasonics* (1998), pp. 925-31 (noting acoustic path length as being equivalent to gasket thickness) (Tab A).

Hence, the thickness of the second wall as claimed by Applicants is equivalent to the path length of the standing wave in the second wall, which is a multiple of about 1/2 the wavelength of the sound wave therein. By contrast, the thickness of the second wall of the device of the Trampler patent is an ***odd*** multiple of 1/4 the wavelength of the sound wave therein (*i.e.* 1/4, 3/4, 5/4, as correctly calculated by the Examiner). ***The Trampler patent thus fails to disclose at least this feature of Applicants' claimed invention.***

Moreover, the Trampler patent affirmatively teaches ***away*** from configuring the thickness of the second wall to be a multiple of 1/2 wavelength of the sound wave therein. According to the Trampler patent, the thickness of the mirror layer forming the second wall should be chosen such that Eigen frequencies of the second wall are avoided. See Trampler, col. 7, ll. 18-23. These Eigen frequencies result from the condition that the phase shift between the surface of the wall has to be a multiple of the number $\pi$, which corresponds to multiples of 1/2 wavelength of the sound wave therein. See id., col. 6, ll. 8-17. As a consequence, the Trampler patent teaches that the thickness of the second wall should ***not*** be a multiple of 1/2 wavelength of the sound wave therein. See id., col. 7, ll. 54-58.

The Hawkes 1 Article wholly fails to cure this deficiency in the Trampler patent. It discloses a separating apparatus comprising a transmission (first) wall and a reflector (second wall), the latter having thickness 5/4 wavelength of the sound wave therein. ***No*** suggestion of configuring the thickness of the second wall to be a multiple of about 1/2 the wavelength of the sound wave therein appears in the Hawkes 1 Article. Accordingly, even were (contrary to fact) the Trampler patent to contemplate modifying its apparatus to be consistent with that of the Hawkes 1 Article, the as-modified device would not be configured as recited in Applicants' claims. For at least these reasons, Applicants request that all rejections of the Examiner be withdrawn.

**Petition for Extension of Time**

Pursuant to 37 C.F.R. § 1.136(a), Applicants petition the Commissioner for all extensions of time needed to respond to the Office Action. Attached behind Tab B is authorization to charge a credit card for $450.00 for the petition fee. Applicants believe no other fee presently is due. However, if Applicants' belief is mistaken, the Commissioner is authorized to debit Deposit Account No. 11-0855 for any additional fee due as a consequence of Applicants' submission of this paper.

## Conclusion

Applicants request that the Examiner allow claims 1-21 and that a patent containing these claims issue in due course.

Respectfully submitted,

Dean W. Russell
Reg. No. 33,452
Attorney for the Assignee

OF COUNSEL:

Kilpatrick Stockton LLP
1100 Peachtree Street
Suite 2800
Atlanta, Georgia 30309
(404) 815-6528

ELSEVIER

Ultrasonics 36 (1998) 925–931

Ultrasonics

# Microparticle manipulation in millimetre scale ultrasonic standing wave chambers

Jeremy J. Hawkes [a,*], David Barrow [a,b], W. Terence Coakley [a]

[a] *School of Pure and Applied Biology, University of Wales Cardiff, Cardiff, CF1 3TL, UK*
[b] *Electronic Engineering Division, School of Engineering, University of Wales Cardiff, Cardiff, CF2 3TF, UK*

Received 28 May 1997

**Abstract**

Ultrasonic standing wave chambers with acoustic pathlengths of 1.1 and 0.62 mm have been constructed. The chambers were driven at frequencies over the range 0.66–12.2 MHz. The behaviour of 2 μm diameter latex microparticles and 5 μm diameter yeast in the chambers has been elucidated. One (flow) chamber had a downstream laminar flow expansion section to facilitate observation of concentrated particle bands formed in the ultrasonic field. A second (microscopy) chamber allowed direct observation of band formation in the field and their characterisation by confocal scanning laser microscopy. Clear band formation occurs when the chamber pathlength is a multiple of half wavelengths at the driving frequency, so that the chamber rather than the transducer resonance has the most influence on band formation in this system. Band formation occurred in half-wavelength steps from a position one quarter of a wavelength off the transducer to a band at a similar distance from the reflector. Ordered band formation was preserved by the laminar flow in the expansion chamber, although bands that formed very close to the wall were dissipated downstream. The microscopy chamber provided evidence of significant lateral particle concentration within bands in the pressure nodal planes. The approaches described will be applicable to the manipulation of smaller particles in narrower chambers at higher ultrasonic frequencies. 

*Keywords:* Ultrasonic radiation force; Micromanipulation; Particle separation; Cell separation

## 1. Introduction

The manipulation of microparticles [1,2] and biological cells [3–6] in standing waves generated by megahertz frequency ultrasonic waves has been investigated in a number of laboratories. Particles, such as cells, which are more dense and less compressible than the suspending phase, migrate under a 'primary' force [7] to pressure nodes separated by half an acoustic wavelength. 'Secondary' forces concentrate particles within the plane of the pressure node and can give rise to localised clumping of particles. The concentrated cells/particles can be removed from suspension by sedimentation in pulsed fields [8], by filtration in a flow system [4,6] or by frequency or phase modulation [5,9].

An essential requirement of the ultrasonic forces, if particles are to be ordered in batch or flowing suspensions, is that they are capable of driving or holding small particles or particle clumps against the thermal currents which are an unavoidable feature of systems subjected to input of energy. Since the primary force is proportional to particle volume, mammalian cells, which have diameters of the order of 20 μm, can be trapped effectively and filtered in a flowing suspension where the standing wave system has an active volume of 75 ml [4]. However, bacteria (with diameters of 1–2 μm) are difficult to manipulate in such large active volumes [8], but have been harvested in smaller (2–8 ml) batch [8] or flow chamber [6] volumes. These smaller scale units may contribute to the clarification of suspensions for supernatant analysis. The scale of sampling and separation required for many analytical techniques continues to decrease [10]. In addition, some ultrasound manipulations e.g. separating particles from the suspending media into one or a small number of discrete streams [11], would be aided by the development of short acoustic path chambers.

The present study attempted to examine how microparticles behave in a short pathlength (0.62–1.1 mm) chamber formed by a plane transducer and reflector.

* Corresponding author.

0041-624X/98/$19.00 
PII: S0041-624X(98)00019-5

The primary force on a particle is proportional to ultrasonic frequency and, consequently, the chambers were driven here over a frequency range of 0.66–12.2 MHz as a prelude to exploiting high frequencies to manipulate submicron particles. Frequencies above 3 MHz also have an advantage in minimising the probability of cavitation so that higher acoustic pressures can be applied to manipulation of smaller particles.

It is difficult to observe particle response in short pathlength chambers when the direction of observation is parallel to the transducer plane [1]. Conditions for particle concentration into bands were identified here by downstream observations of the suspension in a laminar flow expansion chamber where the interband spacing was amplified eightfold [12]. Particle concentration into clumps at the transducer site was monitored through a transparent acoustic reflector. Features of the distribution of particles in the standing wave have been established by observations of fluorescent latex microspheres with a confocal laser scanning microscope. A confocal microscope not only provides sharp images of the planes parallel to the transducer but, by processing the information from serial sections, also constructs a side view of those planes. The approach provides some insight to the near-field pressure distribution in the short pathlength standing wave.

## 2. Materials and methods

### 2.1. Sample preparation

Suspensions of 4.6 μm diameter yeast in distilled water were prepared as previously described [12].

Suspensions of fluorescent 2.16 μm diameter orange beads (Sigma, Ltd.) were diluted in distilled water. Particle concentrations were determined using a bacterial counting chamber (Weber Scientific International).

### 2.2. The acoustic flow chambers

Two acoustic chambers were fabricated. 10 mm wide channels, cut from acetate gaskets, formed the acoustic cavities (Fig. 1). The gaskets were clamped between stainless steel blocks which formed the inlet and outlet channels. In one chamber (expanding laminar flow chamber), bands were viewed side-on after they left the acoustic field [12]. In the second chamber (the microscopy chamber) bands were observed normal to the transducer while still in the acoustic field.

#### 2.2.1. Expanding laminar flow chamber

The gasket thickness (acoustic pathlength) was 1.1 mm. The 10 mm wide chamber (Fig. 1(a)) consisted of four regions:

(1) A 40 mm long laminar flow stabilisation entry region.

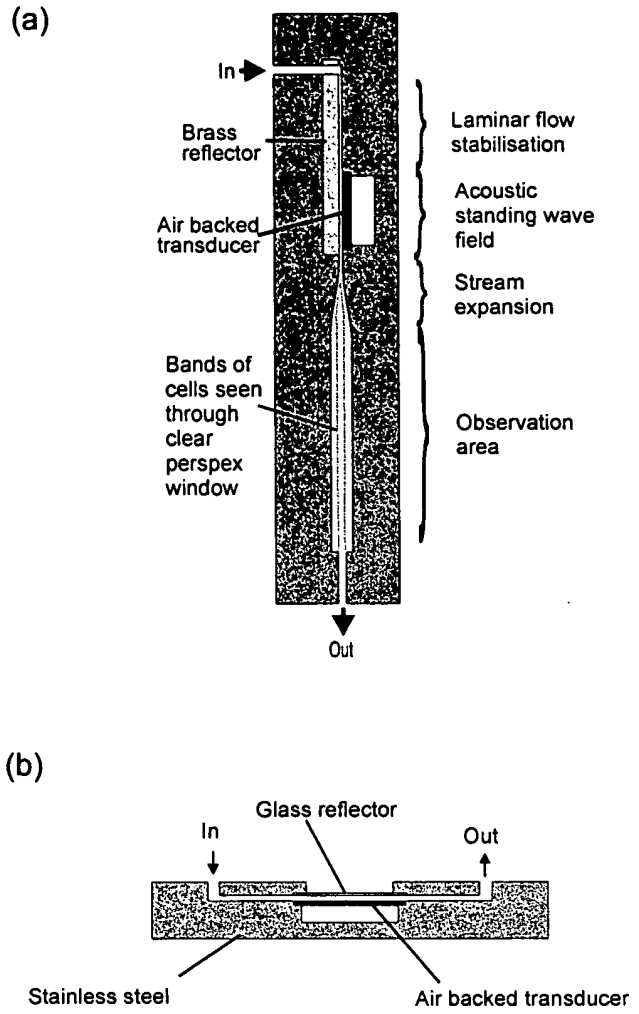


Fig. 1. Schematic diagram of (a) the flow expansion acoustic chamber, with downstream observation of bands and (b) a microscopy chamber with glass reflector for observation of bands.

(2) A 15 mm long ultrasound standing wave field. A 25 mm diameter transducer with a fundamental resonant frequency near 3 MHz formed one wall of the cavity. A 3 mm thick brass block formed the reflector. Ultrasound generation was restricted to the acoustic cavity by etching the back electrode to 10 × 15 mm.

(3) A 30 mm long 6.6° gentle taper flow expansion (1.1–8 mm) region.

(4) A 65 mm long observation window.

Whilst the chamber was in operation it was held vertically, with fluid flowing downwards as in Fig. 1(a). Suspensions were drawn through the chamber by a peristaltic pump (Gilson minipuls 3) at flow rates up to 0.1 ml $s^{-1}$.

#### 2.2.2. The microscopy chamber

The channel acetate gasket thickness was either 1.1 or 0.62 mm. An air-backed 20 × 20 mm PZT 26 plate

transducer (Ferroperm, Krisgard, Denmark), with a fundamental thickness resonant frequency near 3.6 MHz, formed one wall, while a glass sheet (1.2 mm thick) formed the reflecting wall. The transducer faces were etched to form central strip electrodes (15 × 3 mm) on the front and back of the transducer. The strips were at right angles to each other and crossed at the centre of the transducer so that ultrasound generation was restricted to a central 3 × 3 mm area of the acoustic cavity. Electrical connection was made with silver-loaded paint (Agar Scientific Ltd.) to the ends of the electrode strips, far away from the active centre of the transducer.

Samples were normally injected into the microscopy chamber where observations were made on static systems. In a number of cases (described in Section 3) samples were drawn through the chamber by a peristaltic pump. The particles, concentrated in bands at pressure nodes, were viewed at right angles to the transducer face through the glass reflector.

### 2.3. Transducer drive

The transducers were driven by a voltage from an amplifier (Model A150, ENI, Rochester, NY). The frequency dependence of amplifier output voltage (reflecting load impedance) was established by sweeping the frequency synthesizer (HP 3326A) input to the amplifier. In routine operations, the maintenance of selected cavity resonances was computer controlled [13]. In some cases the microscopy chamber transducer was driven directly by the frequency synthesizer.

### 2.4. Video observation

Video images (macro zoom lens, Fujitsu colour camera, Sony VHS Combo) were recorded at the observation area of the expanding chamber or the glass reflector of the microscopy chamber.

### 2.5. Confocal microscopy

Band formation in the microscopy chamber standing wave was observed with a confocal laser scanning microscope (Molecular Dynamics, Sarastro 2000 with Image Space software run on Silicon graphics workstations). Orange fluorescent beads within the chamber and the reflective silver transducer electrode at the base of the chamber were detected separately using dual channel scanning, laser fluorescence and reflectance mode. The excitation, detection and secondary beam splitter wavelengths were 488, 510 and 565 nm respectively. A × 10 objective was used throughout. The field was scanned at vertical intervals of 10 μm. Images were constructed from 120 such scans of sections through the 1.1 mm deep chamber and the reflector. The scanning time for the series was approximately 20 min. Low transducer voltages were therefore used to minimise alterations to the banding pattern over this long period. The images were obtained with a static suspension as particles with velocities greater than a few micrometers per second could not be detected. The microscope's digital image processing capability permits construction of views at right angles to the original microscope view and thus provides images both in the plane of the bands and at right angles to those planes.

## 3. Results

### 3.1. Particle band formation at cavity resonances

A frequency sweep of the voltage applied to the expansion chamber transducer, for a fixed amplifier input voltage, is shown in Fig. 2. The principal minimum occurs at the transducer fundamental thickness resonance of 2.98 MHz. The identification of some of the secondary minima as cavity thickness resonances was carried out as follows: a yeast suspension was drawn through the expansion chamber (Fig. 1(a)) and the driving frequency was slowly varied over the frequency range 0.3–7 MHz. The suspension, which had passed through the standing wave field, was viewed through the side observation window (Fig. 1(a)). A single diffuse band was seen at the cavity fundamental resonance of 0.66 MHz. Two and three sharp bands were seen at the second and third harmonic of the cavity resonance frequency, respectively. The banding pattern was lost at frequencies between cavity resonances. An example of banding pattern, at 1.96 MHz, is shown in Fig. 3. The frequency at which discrete bands appeared in the outflow from the standing wave coincided with the voltage minima marked on Fig. 2. Dips in the voltage were seen at all frequencies where bands occurred, but limitations of the graphics resolution obscure some minima in Fig. 2. No bands appeared at the transducer resonance (the principal minimum) of Fig. 2.

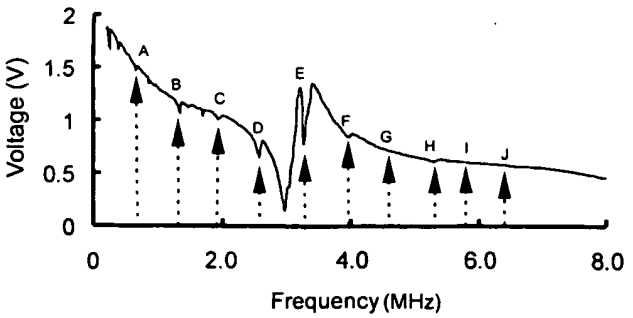


Fig. 2. The variation in transducer driving voltage with frequency. The amplifier input was constant at 20 $mV_{p-p}$. The lettered arrows indicate frequencies where band formation was observed (see text and Table 1).

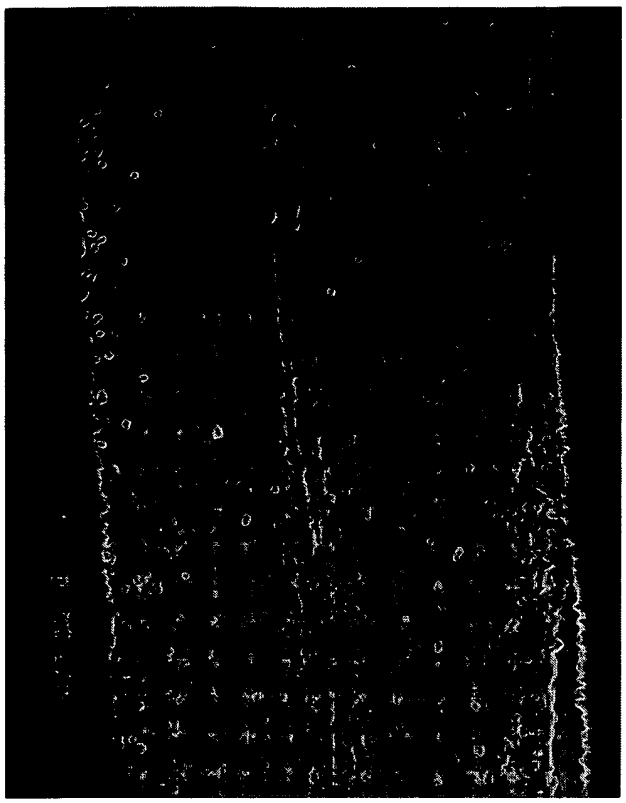

Fig. 3. The band pattern observed downstream when the amplifier was driven with a 70 $mV_{p-p}$ signal at 1.96 MHz. A suspension of $5 \times 10^6$ yeast cells per ml had passed through the sound field at a flow rate of 0.1 ml $s^{-1}$.

The ultrasonic frequencies at which bands were observed are shown in Table 1. The increment between each of the band-forming frequencies were of similar magnitude (Table 1) so that each resonance was close to an integral multiple of the fundamental cavity resonance frequency. The number of bands observed and the number expected on the basis of harmonics of the cavity resonance are also shown. The number of bands appearing in the channel was less than the number expected at the 5th harmonic and above. We attribute this loss of bands to dissipation of slowly moving bands at the edges of the channel.

Table 1
The transducer frequencies at which bands appeared in the expanding chamber system. A suspension of $5 \times 10^6$ yeast cells per ml had been pumped through the sound field at a flow rate of 0.1 ml $s^{-1}$

| | Frequency (kHz) | Δ frequency (kHz) | Number of half wavelengths | Number of bands observed |
|---|---|---|---|---|
| A | 662.5 | | 1 | 1 |
| B | 1337.5 | 675.0 | 2 | 2 |
| C | 1969.5 | 632.0 | 3 | 3 |
| D | 2584.0 | 614.5 | 4 | 4 |
| E | 3273.0 | 689.0 | 5 | 3 |
| F | 3966.0 | 693.0 | 6 | 4 |
| G | 4596.0 | 630.0 | 7 | 5 |
| H | 5310.0 | 714.0 | 8 | 5 |
| I | 5815.0 | 694.0 | 9 | 6 |
| J | 6445.0 | 609.0 | 10 | 6 |

The microscopy chamber resonances were identified, in the light of the above results for the expansion chamber, by the small regularly spaced minima on the voltage frequency spectrum.

### 3.2. Particle distribution in the microscopy chamber standing wave

#### 3.2.1. Formation of columns and clumps

Video observations of yeast suspensions ($3 \times 10^8$ ml $^{-1}$) drawn at 0.02 ml $s^{-1}$ (average flow velocity 3 mm $s^{-1}$) through the 0.62 mm pathlength microscopy chamber were carried out through the reflector window (Fig. 1(b)). Band formation could not be viewed from this perspective, but patterns of particle concentration in planes parallel to the transducer could be observed when the transducer was driven at relatively high voltages, of the same order as those applied to form the band patterns of Fig. 2 in the expanding flow chamber.

A column of clumps of yeast cells formed from the flowing suspension and trapped in the standing wave column of yeast cells is shown in Fig. 4(a). The column appears as a single clump from the overhead camera perspective. The clumps reached their maximum size within 2 s. Real-time observation showed that cells continue to be attracted to the column as they flow in from the right of the field, and cells are lost from the clump in flow to the left. This equilibrium state continues indefinitely when the suspension contains a low (ca. $10^{-3}$ w/v) biomass concentration. At higher concentrations, the column becomes unstable and clumps break away (sometimes the whole column is lost). The column then reforms. This formation and break-up of the column often has a regular periodicity of a few seconds.

The column is lost as clumps move downstream when the sound is switched off (Fig. 4(b)). The parabolic profile of the flow combined with the tendency to sediment on termination of the ultrasound exposed the four component clumps. The presence of four clumps is consistent with the fact that the transducer had been driven at the fourth harmonic of the cavity resonance.

### 3.3. Position of bands within the ultrasonic field

Standing waves were set up in the 1.1 mm pathlength microscopy chamber, and the distribution of fluorescent latex beads (2.16 μm diameter) in a non-flowing suspension was observed with a confocal microscope. A low drive voltage (0.6 $V_{p-p}$) was applied directly from the signal generator to the transducer in order to accommodate the long time (20 min) required to complete the 120 scans contributing to the confocal image. The individual bands are clearly seen (Fig. 5(a),(c)) when

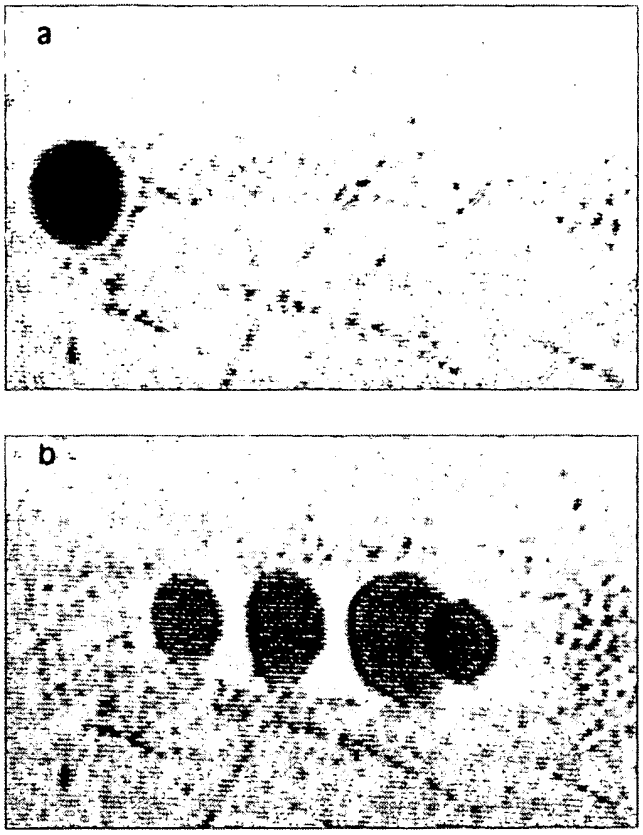


Fig. 4. A yeast suspension flowing through a 0.62 mm pathlength microscopy chamber at 0.02 ml $s^{-1}$ and observed along the axis of the sound beam: (a) A column of cell clumps, formed in the flow and trapped in the standing wave, 20 s after 'sound on'; (b) 2 s after 'sound off' the four sedimenting clumps of the column have separated as the parabolic velocity-profile flow carries them downstream at different rates. The transducer was driven by 12 $V_{p-p}$ at a 4th harmonic cavity resonance of 4.8 MHz.

the image is reconstructed at right angles to the original microscope view. The interband spacing is 183 μm (half a wavelength) for the conditions of Fig. 5(a). The distance of the closest band from the reflector was about 90 μm, i.e. a quarter wavelength. Other scans showed that the distance of the closest band from the transducer was also a quarter wavelength. Some particles have collected on the glass reflector in Fig. 5(a) and on the transducer in Fig. 5(c). Some of these particles appear yellow; the fluorescence and reflectance signals are presented as red and green, respectively while a combination of these signals is presented as a yellow image. The micrograph of Fig. 5(b) shows the same field where the data is integrated in the vertical plane. Individual sections among the 120 integrated for Fig. 5(b) emphasise the discrete clumps forming at different levels more clearly.

Band and intraband clump formation are shown at the higher frequency of 12.2 MHz in Fig. 5(c). 'Column' formation of clumps is also seen on the left of the image. Fig. 5(d) shows the same field where the data is integrated in the vertical plane.

## 4. Discussion

The requirement in the present systems to drive the chamber at its thickness resonance or at a harmonic in order to form bands was established by the observation that bands appeared in the flow expansion chamber only at frequencies at which the amplifier load was an impedance minimum. This result helped identify the frequencies at which band formation was expected (and was later confirmed by confocal microscopy) in the microscopy chamber, where direct lateral observation of bands was not possible.

Confocal microscopy also showed that the bands closest to the transducer and the reflector were spaced at a quarter wavelength from those surfaces. The observation is consistent with the presence of pressure antinodes at the surfaces where, for both cases, the specific acoustic impedance of the solid is greater than that of the liquid [14]. Some particles were also detected on both the transducer and reflector. Those on the transducer might have arisen from clump sedimentation under gravity but it is not possible to account for the particles on the reflector in this way.

The number of bands in a standing wave was expected to increase linearly with the order of the chamber harmonic as the frequency was increased. Confocal microscopy confirmed that this was indeed the case for the microscopy chamber (Fig. 5(a),(c)) where the suspension was static and the transducer drive voltage was low. The relationship also held up to the fourth harmonic (2.58 MHz) for the suspension flowing in the expansion chamber (Table 1). At 2.58 MHz, four bands formed, the outer two being 0.143 mm from the chamber wall. At all higher frequencies the bands which formed at less than this distance from the walls were not seen in the observation window. This result suggests that all bands observed were formed in the central 74% of the acoustic path. The Reynolds number of water flowing at 10 mm $s^{-1}$ in a 1.1 mm wide channel is 5, so that laminar flow would be expected in the acoustic chamber. The velocity $u_x$ of laminar flow at a distance $s$ from the centre of a channel is given by $u_x=(6/d^3)(Q')(d^2/4-s^2)$, where $Q'$ is the average volume flow rate through a channel of unit width and $d$ is the channel depth. Integration of this equation with respect to $s$ shows that only 9% of the flowing volume falls within 0.14 mm of the chamber walls. The loss of bands (band dissipation) at the higher chamber harmonics may have arisen from gravitational sedimentation of particle clumps through those bands moving downstream most slowly at the chamber wall or to local

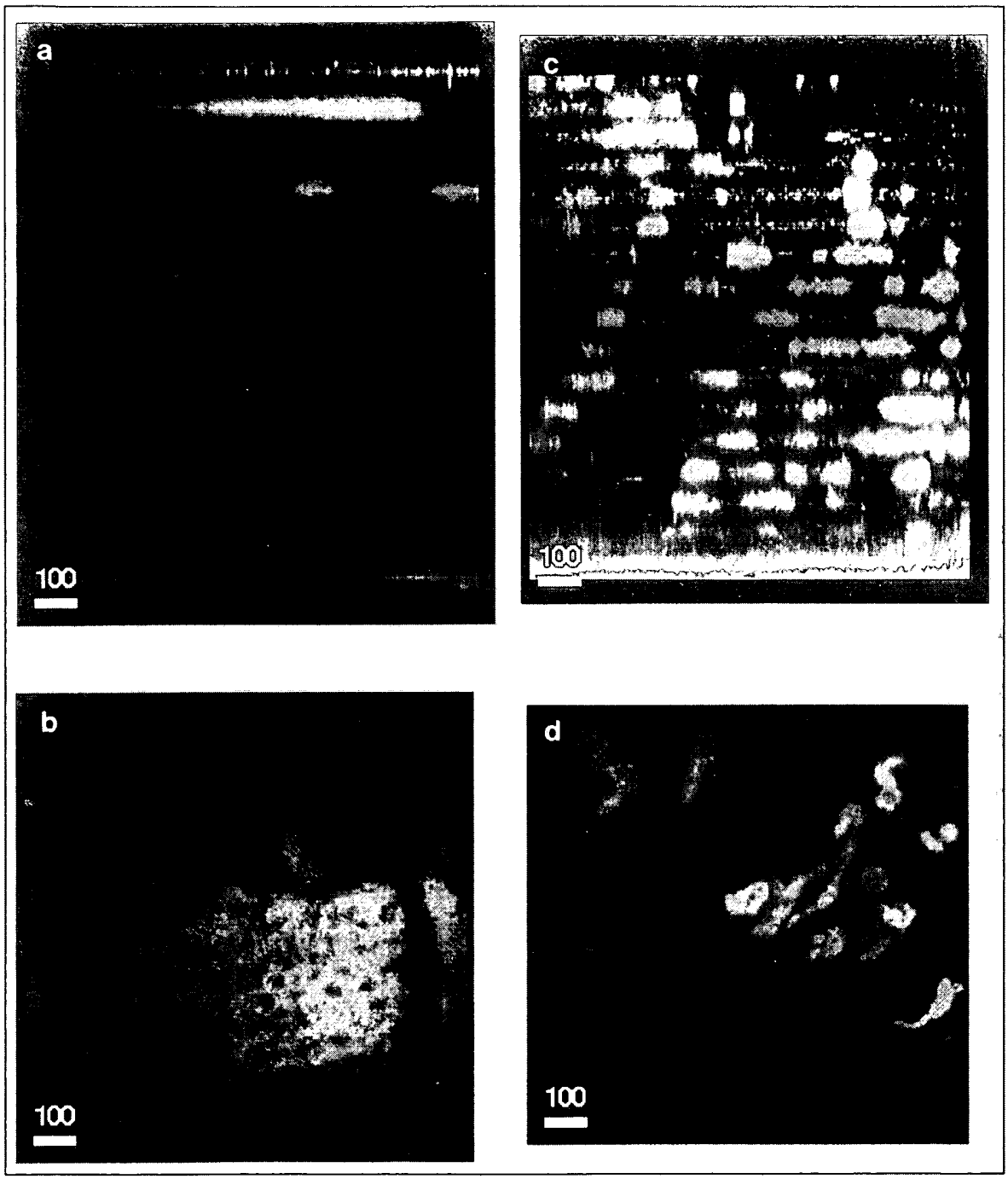


Fig. 5. Reconstructed (integrated) confocal micrographs of 2.16 μm diameter fluorescent orange latex particles ($5.6 \times 10^8$ ml$^{-1}$) in the 1.1 mm thick microscopy chamber (a),(b) 4.08 MHz frequency (6th harmonic of cavity resonance), transducer voltage, 0.6 $V_{p-p}$; (c),(d) 12.2 MHz frequency, driving voltage 1.2 $V_{p-p}$. Image planes (a),(c) parallel to the sound axis; (b),(d) normal to the sound axis.

laminar flow disruption due to some residual roughness of the chamber walls and junctions.

The concentration of particles within the plane of the confocal microscopy bands generated at low transducer voltages reflects local velocity antinode maxima. The confocal microscopy technique therefore has the potential to provide further insight to the fine structure of the near field in short pathlength chambers. Particles formed a single column of large clumps (Fig. 4) at the high voltages of the same magnitude as those applied to generate the particle distribution in the downstream laminar flow of Fig. 3. A rhythmic pattern of large clump formation and loss was directly observed when high concentrations of yeast were drawn through the microscopy chamber. A similar phenomenon was implied in the expansion chamber where a rhythmic

change of band thickness was seen in the downstream expanding chamber when high yeast concentrations were used.

The picture which emerges of fine particle behaviour in mini-chambers is of

(1) band formation in half-wavelength steps from a position one quarter of a wavelength off the transducer to a band at a similar distance from the reflector;
(2) concentration of particles into clumps in the plane of the band at low drive voltage;
(3) convergence of these clumps in the plane of the bands at higher voltages but maintenance of the half wavelength clump separation normal to the nodal planes.

Frequencies up to 12 MHz, a chamber of 0.62 mm pathlength and behaviour of particles of 2 μm diameter have been characterised in this work. Further developments with higher frequencies, smaller chambers and particles are clearly feasible.

## Acknowledgement

The authors are grateful to Bethan Hill for the confocal microscope pictures and to Howard Williams for construction of the chambers. The work was supported by EPSRC Grant GR/L15531.

## References

[1] Z.I. Mandralis, D.L. Feke, R.J. Adler, Transient response of fine particle suspensions to mild planar ultrasonic fields, Fluid Particle Sep. J. 3 (1990) 115.
[2] K. Higishitani, M. Fukushima, Y. Matsuno, Migration of suspended particles in plane stationary ultrasonic fields, Chem. Eng. Sci. 36 (1981) 1187.
[3] F. Trampler, S.A. Sonderhoff, W.S. Pui, D.G. Kilburn, J.M.W. Piret, Acoustic cell filter for high density perfusion culture of hybridoma cells, Bio/Technol. 12 (1994) 281.
[4] O. Doblhoff-Dier, Th. Gaida, H. Katinger, W. Burger, M. Groschl, E. Benes, A novel ultrasonic resonance field device for the retention of animal cells, Biotechnol. Prog. 10 (1994) 428.
[5] S. Peterson, G. Perkins, C. Baker, Development of an ultrasonic blood separator, Proc. IEEE 8th Conf. Eng. Med. Biol. Soc., 1986, p. 154.
[6] J.J. Hawkes, M.S. Limaye, W.T. Coakley, Filtration of bacteria and yeast by ultrasound-enhanced sedimentation, J. Appl. Micro. 82 (1997) 39.
[7] R.E. Apfel, Acoustic radiation pressure – principles and applications to separation science. Fortsh. Akust. DAGA '90 S., 1990, p. 19.
[8] M.S. Limaye, J.J. Hawkes, W.T. Coakley, Ultrasonic standing wave removal of microorganisms from suspension in small batch systems, J. Microbiol. Meth. 27 (1996) 211.
[9] G. Whitworth, M.A. Grundy, W.T. Coakley, Transport and harvesting of suspended particles using modulated ultrasound, Ultrasonics 29 (1991) 439.
[10] S.J. Haswell, Development and operating characteristics of micro flow injection analysis systems based on electroosmotic flow – a review, Analyst 122 (1997) R1.
[11] K. Yasuda, S.-I. Umemura, K. Takeda, Concentration and fractionation of small particles in liquid by ultrasound, Jpn. J. Appl. Phys. 34 (1995) 2715.
[12] J.J. Hawkes, D. Barrow, J. Cefai, W.T. Coakley, A laminar flow expansion chamber facilitating downstream manipulation of particles concentrated using an ultrasonic standing wave, Ultrasonics 36 (1998) 901.
[13] J.J. Hawkes, W.T. Coakley, A continuous flow ultrasonic cell-filtering method, Enzyme and Microb. Tech. 19 (1996) 57.
[14] V.A. Shutilov, Fundamental Physics of Ultrasound (Translated from Russian by M.E. Alferieff), Gordon and Breach, New York, 1988, p. 183.